

# Nanoporous Gold Catalyst for Highly Selective Semihydrogenation of Alkynes: Remarkable Effect of Amine Additives

Mei Yan,<sup>†</sup> Tienan Jin,<sup>\*,†</sup> Yoshifumi Ishikawa,<sup>†</sup> Taketoshi Minato,<sup>‡,||</sup> Takeshi Fujita,<sup>†</sup> Lu-Yang Chen,<sup>†</sup> Ming Bao,<sup>§</sup> Naoki Asao,<sup>†</sup> Ming-Wei Chen,<sup>†</sup> and Yoshinori Yamamoto<sup>†,§</sup>

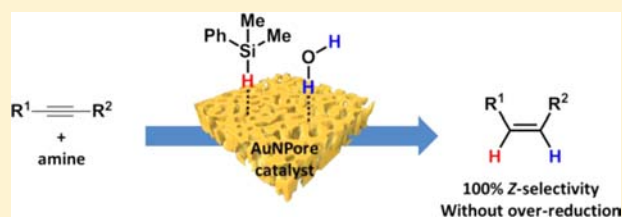
<sup>†</sup>WPI-Advanced Institute for Materials Research (WPI-AIMR), Tohoku University, Sendai 980-8577, Japan

<sup>‡</sup>Institute for International Advanced Interdisciplinary Research (IIAIR), International Advanced Research and Education Organization, Tohoku University, Sendai, 980-8578, Japan

<sup>§</sup>State Key Laboratory of Fine Chemicals, Dalian University of Technology, Dalian 116012, China

## S Supporting Information

**ABSTRACT:** We report for the first time the highly selective semihydrogenation of alkynes using the unsupported nanoporous gold (AuNPore) as a catalyst and organosilanes with water as a hydrogen source. Under the optimized reaction conditions, the present semihydrogenation of various terminal- and internal-alkynes affords the corresponding alkenes in high chemical yields and excellent Z-selectivity without any over-reduced alkanes. The use of DMF as solvent, which generates amines in situ, or pyridine as an additive is crucial to suppress the association of hydrogen atoms on AuNPore to form H<sub>2</sub> gas, which is unable to reduce alkynes on the unsupported gold catalysts. The AuNPore catalyst can be readily recovered and reused without any loss of catalytic activity. In addition, the SEM and TEM characterization of nanoporosity show that the AuNPore catalyst has a bicontinuous 3D structure and a high density of atomic steps and kinks on ligament surfaces, which should be one of the important origins of catalytic activity.



## INTRODUCTION

Catalysis using unsupported nanoporous gold (AuNPore) materials has attracted increasing interest due to their potentially green and sustainable catalytic properties.<sup>1–3</sup> The monolithic AuNPore can be fabricated by selective leaching of Ag from Au–Ag alloy.<sup>4</sup> The interesting features of AuNPore, such as three-dimensional (3D) bicontinuous open pore network structure, high surface-to-volume ratio in comparison with bulk metals, distinguished electronic property, nontoxic nature, high recyclability, and rather simple recovery, make it an attractive candidate for new heterogeneous catalyst. Moreover, in contrast to the supported gold nanoparticles (AuNPs),<sup>5</sup> AuNPore without supports should be a challenging catalyst system to understand the intrinsic catalytic activity more easily and to extend the catalytic application widely by elimination of the support-effect problems and relaxation of aggregation.<sup>6</sup>

Recent advances on catalytic applications using AuNPore catalyst, such as gas-phase CO oxidation and MeOH oxidation, liquid-phase oxidation of alcohols and glucose, as well as electrochemical oxidation of MeOH, demonstrated its excellent activity for selective oxidation reactions.<sup>1–3</sup> However, AuNPore catalyst has not been used for selective hydrogenation so far because of the limited ability of H<sub>2</sub> dissociation of gold as compared to its counterpart of the Pd group metals.<sup>7</sup> The HD formation studies using the TiO<sub>2</sub> supported AuNPs indicated that the small size of AuNPs and the gold/metal oxide interface play an important role for H<sub>2</sub> dissociation;<sup>8</sup> thus, it is not surprising that

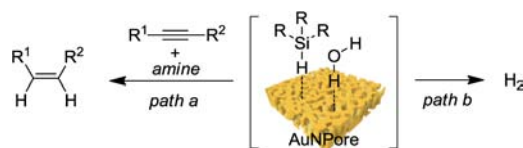
the hydrogenation reaction using the unsupported AuNPore as a catalyst is still unsuccessful.

Although some efficient homogeneous catalytic systems are known for the semihydrogenation of alkynes,<sup>9</sup> the development of a highly active and selective heterogeneous catalyst for this reaction would be highly desirable from the point of view of organic synthesis and industrial interest. Heterogeneous catalysis based on Pd and Ni metals has been studied extensively to reduce alkynes to Z-alkenes with H<sub>2</sub> but suffer from E/Z isomerization and over-reduction of alkenes.<sup>10</sup> It was reported that the supported AuNPs catalysts are unique in the gas-phase hydrogenation of alkynes with H<sub>2</sub>, producing the corresponding alkenes with almost perfect selectivity due to the stronger adsorption of the alkynes as compared to the alkenes, but the activity was poorer than that of PdNPs.<sup>11</sup> Most recently, our group reported that AuNPore was an effective catalyst for oxidation of organosilanes with water without any additives, producing organic silanols in high yields along with the vigorous liberation of H<sub>2</sub> gas (Scheme 1, path b).<sup>12a</sup> In the continuation of our interest in the development of new catalyst properties of nanoporous metals,<sup>2b,12</sup> herein, we report for the first time the highly selective semihydrogenation of alkynes catalyzed by the unsupported nanoporous gold using amines as an additive and organosilanes with water as a hydrogen source, affording the

Received: May 16, 2012

Published: October 1, 2012

### Scheme 1. AuNPore-Catalyzed Selective Semihydrogenation of Alkynes Using Hydrosilanes and H<sub>2</sub>O as H<sub>2</sub> Source



corresponding alkenes in excellent *Z*-selectivity without any over-reduced alkanes (Scheme 1, path a).

## RESULTS AND DISCUSSION

**Nanoporosity Characterization of AuNPore.** The unsupported AuNPore catalyst was prepared by dealloying of a homogeneous Au<sub>30</sub>Ag<sub>70</sub> alloy with thickness of 40 μm in 70 wt % of nitric acid as an electrolyte at room temperature for 18 h.<sup>12a</sup> The scanning electron microscopy (SEM) image in Figure 1a shows that ligaments and nanopore channels are

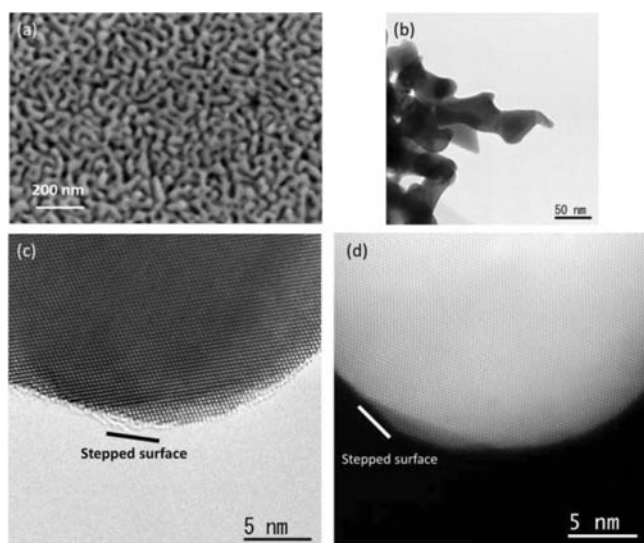


**Figure 1.** (a) SEM image of AuNPore, (b) representative bright-field TEM image, (c) HRTEM image with stepped surface, and (d) HAADF-STEM image with stepped surface.

formed uniformly across the entire AuNPore with an average ligament size around 30 nm. Energy dispersive X-ray (EDX) study shows that the residual Ag composition of AuNPore is 2% (see Figure S1a). Figure 1b shows the representative bright-field transmission electron microscopy (TEM) image of AuNPore, which clearly reveals the multiple layers of gold ligaments with convex and concave columnar curvatures, indicating that the nanoporous structure is a bicontinuous 3D network. Moreover, the ligament size is determined to be about 30 nm, which is consistent with the values estimated from the SEM image. Characterization of a convex region of ligament with high-resolution TEM (HRTEM) and scanning TEM (STEM) mode with high-angle annular dark-field (HAADF) detector shows a very high density of atomic steps and kinks at curved surfaces (Figure 1c and d), implying the presence of a high concentration of low-coordination surface atoms. As the most recent observations on CO oxidation with AuNPore catalyst analyzed by in situ environmental HRTEM clearly indicated that the high density of low-coordination atoms on surface are the catalytically active sites,<sup>6</sup> we predict that the obvious surface

defects of AuNPore might be one of the most important origins of the catalytic activity in the present hydrogenation.<sup>13</sup>

To gain more insight into the origin of catalytic property, the chemical state of AuNPore was measured by X-ray photoelectron spectroscopy (XPS). Analysis of AuNPore shows that AuNPore is composed of Au and Ag, while Au is predominant component. The difference of binding energy of Au 4f 7/2 between AuNPore (84.1 eV) and Au mica (84.0 eV) is very small, from which it can be concluded that the electronic states of AuNPore and Au mica are the same (Figure 2a vs b). This

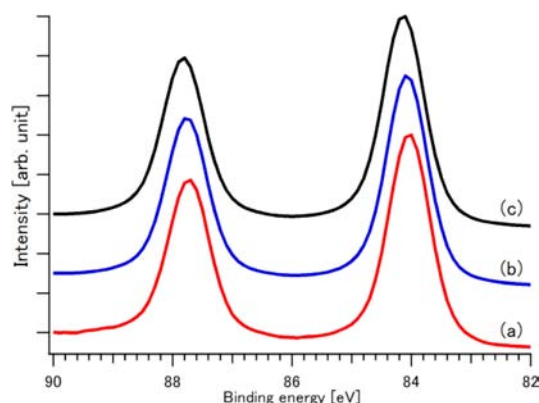


**Figure 2.** Normalized XPS spectra of (a) Au mica (red), (b) fresh AuNPore (blue), and (c) AuNPore treated with pyridine (black, see the control experiments section).

suggests that AuNPore is metallic gold(0) that is playing as the catalytic species in the present reaction.

**AuNPore-Catalyzed Oxidation of Organosilanes with Water.** As aforementioned, recently, we observed that AuNPore has a remarkable catalytic activity in the oxidation of organosilanes with water, forming the corresponding silanols together with the evolution of hydrogen gas.<sup>12a</sup> The reaction proceeds efficiently at room temperature without any formation of disiloxanes, and a wide range of organosilanes are compatible with the mild reaction systems. For example, as shown in Table 1, not only aromatic silanes but also sterically less-hindered and hindered trialkylsilanes were oxidized effectively. The AuNPore catalyst was also applicable to the oxidations of tri-, di-, and monophenylsilanes, and the corresponding oxygenated products were obtained in high yields, respectively.

Taking the mechanism into consideration, we assumed that H<sub>2</sub> gas should be produced through the association of the in situ generated hydrogen atoms on AuNPore (Scheme 1, path b). If this is the case, we can imagine that the catalytic hydrogenation of the unsaturated multiple bonds such as alkynes by the hydrogen atoms on AuNPore should be achieved through the suppression of the quick association of these hydrogen atoms (Scheme 1, path a).

**Optimization of AuNPore-Catalyzed Semihydrogenation of Phenyl Acetylene with Various Organosilanes and Water Using DMF as Solvent (Method A).** In the preliminary experiment, we found that the hydrogenation of phenylacetylene **1a** with H<sub>2</sub> in organic solvents by using AuNPore as a catalyst did not proceed at all (Table 2, entry 1). On the basis of the organosilane oxidation conditions and the new hypothesis, initially **1a** was treated with AuNPore catalyst, PhMe<sub>2</sub>SiH, and water in the presence of various organic solvents including acetone, CH<sub>2</sub>Cl<sub>2</sub>, THF (tetrahydrofuran), toluene, acetonitrile, and DMF (dimethylformamide). Surprisingly, only the

Table 1. AuNPore-Catalyzed Oxidation of Organosilanes with Water<sup>a</sup>

entry	R <sub>(4-n)</sub> SiH <sub>n</sub>	mol % (AuNPore)	t (h)	yield (%) <sup>b</sup> (R <sub>(4-n)</sub> Si(OH) <sub>n</sub> )
1	Et <sub>3</sub> SiH	1	2	94
2	Bu <sub>3</sub> SiH	3	3	95
3	( <i>i</i> -Pr) <sub>3</sub> SiH	3	5	98
4	PhMe <sub>2</sub> SiH	1	1	100
5	Ph <sub>3</sub> SiH	1	5	99
6	Ph <sub>2</sub> SiH <sub>2</sub>	1	9	90
7	PhSiH <sub>3</sub>	5	6	80

<sup>a</sup>Reaction conditions: organosilanes (1 mmol), H<sub>2</sub>O (0.1 mL), and AuNPore (1–5 mol %) in 1.5 mL of acetone at room temperature. <sup>b</sup>Isolated yield.

Table 2. Screening of the Reaction Conditions Using DMF as Solvent<sup>a</sup>

entry	catalyst	R <sub>3</sub> SiH	2a (%) <sup>b</sup>
1	AuNPore	H <sub>2</sub> (1 atm) <sup>c</sup>	0
2	AuNPore	PhMe <sub>2</sub> SiH	96 (96, <sup>d</sup> 98 <sup>e</sup> )
3	AuNPore	HMe <sub>2</sub> SiOSiMe <sub>2</sub> H	85
4	AuNPore	Et <sub>3</sub> SiH	79
5	AuNPore	( <i>n</i> -Bu) <sub>3</sub> SiH	47
6	AuNPore	( <i>i</i> -Pr) <sub>3</sub> SiH	9
7	AuCl	PhMe <sub>2</sub> SiH	18
8	Au <sub>30</sub> Ag <sub>70</sub> alloy	PhMe <sub>2</sub> SiH	0
9	none	PhMe <sub>2</sub> SiH	0
10 <sup>f</sup>	PdNPore	PhMe <sub>2</sub> SiH	54
11 <sup>g</sup>	Pd/C	PhMe <sub>2</sub> SiH	20

<sup>a</sup>Conditions: To a DMF solution (0.5 mL) of AuNPore (2 mol %) were added **1a** (0.5 mmol), H<sub>2</sub>O (1 mmol), and PhMe<sub>2</sub>SiH (0.75 mmol). The resulting mixture was stirred at 35 °C for 2 h. <sup>b</sup><sup>1</sup>H NMR yield determined using anisole as an internal standard. For the yields lower than 96%, some amounts of **1a** remained without formation of the over-reduced alkane. <sup>c</sup>H<sub>2</sub> gas (1 atm) was used instead of PhMe<sub>2</sub>SiH. <sup>d</sup>The yield of second use. <sup>e</sup>The yield of third use. <sup>f</sup>PdNPore was prepared from PdAl alloy. <sup>g</sup>The particle size was 5 nm.

use of DMF as solvent afforded the corresponding styrene **2a** in high yield (entry 2), and other solvents were almost ineffective, giving **2a** in less than 10% yield. The AuNPore catalyst was recovered by simply picking the skeleton catalyst up and was reused for another two runs without any loss of catalytic activity (entry 2, in parentheses). In addition, the SEM image in Figure S1b showed that no significant changes of the nanoporous structure of AuNPore were observed after the third run. Further examination of other organosilanes using DMF as solvent showed that the steric hindrance of substituents on silicon exhibited a significant influence on reaction efficiency; for example, 1,1,3,3-tetramethyldisiloxane was still active, giving **2a** in 85% yield, whereas with the use of triethylsilane, tributylsilane, and triisopropylsilane, respectively, the yield of **2a** was decreased dramatically (entries 3–6). The homogeneous gold catalyst such as AuCl did not show a good catalytic activity (entry 7). It was noted that the reaction with the AuNPore precursor, Au<sub>30</sub>Ag<sub>70</sub> alloy as a catalyst, or without catalyst did not proceed (entries 8 and 9). Other catalysts such as nanoporous palladium (PdNPore) and Pd/C are also active, but the yields are much lower than that with AuNPore (entries 10 and 11).

**Optimization of Amine Additives on AuNPore-Catalyzed Semihydrogenation (Method B).** The remarkable solvent effect in the present reaction led us to investigate the detailed role of DMF. During the reaction in DMF, we observed a foul odor from reaction mixture, which seems to be Me<sub>3</sub>N or Me<sub>2</sub>NH.<sup>14</sup> Consequently, *N*-methyl-*N*-phenylformamide (Ph(Me)NCHO) was used instead of DMF under method A. The <sup>1</sup>H NMR and gas chromatography (GC–MS) analysis showed the formation of a mixture of *N*-methyl-*N*-phenylamine (PhNHMe) and *N,N*-dimethyl-*N*-phenylamine (PhNMe<sub>2</sub>), which clearly indicated that amines generated in situ from DMF might play an important role in the semihydrogenation of alkynes. To gain further insight into the role of amines, we examined various amines (0.5 equiv) in the absence of DMF (Table 3). As expected, semihydrogena-

Table 3. Screening of the Amine Additives for Semihydrogenation of Dodec-1-yne **1b**<sup>a</sup>

entry	amine	amount of amine (equiv)	2b (%) <sup>b</sup>
1	PhNHMe	0.5	72
2	PhNMe <sub>2</sub>	0.5	57
3	Et <sub>2</sub> NH	0.5	69
4	Et <sub>3</sub> N	0.5	11
5	pyridine	0.5	84
6	none	0	7
7	pyridine	0.2	78
8	pyridine	1.0	98
9	pyridine	1.5	81
10 <sup>c</sup>	pyridine	1.0	98

<sup>a</sup>Reaction conditions: To a CH<sub>3</sub>CN solution (0.5 mL) of AuNPore (2 mol %) were added **1b** (0.5 mmol), H<sub>2</sub>O (1 mmol), base (0.25 mmol), and PhMe<sub>2</sub>SiH (0.75 mmol). The resulting mixture was stirred at 80 °C for 10 h. <sup>b</sup><sup>1</sup>H NMR yield determined using anisole as an internal standard. For the yields lower than 84%, some amounts of **1b** remained without formation of the over-reduced alkane. <sup>c</sup>AuNPore (0.2 mol %) was used, and the reaction time was 45 h.

tion of the dodec-1-yne **1b** with PhNHMe or PhNMe<sub>2</sub> as a base in acetonitrile at 80 °C gave the corresponding dedec-1-ene **2b** in 72% and 57% yields, respectively (entries 1 and 2). It seems that amines with a lower basicity exhibit a higher activity; for example, the use of Et<sub>2</sub>NH gave a higher yield of **2b** than did Et<sub>3</sub>N (entries 3 and 4). Finally, we found that when pyridine was used, the yield of **2b** was increased up to 84% yield together

Table 4. AuNPore-Catalyzed Semihydrogenation of Various Alkynes<sup>a</sup>

Method A: DMF as solvent  
 Method B: pyridine, CH<sub>3</sub>CN as solvent

**1a:** R<sup>1</sup> = C<sub>6</sub>H<sub>5</sub>, R<sup>2</sup> = H

**1b:** R<sup>1</sup> = *n*-C<sub>10</sub>H<sub>21</sub>, R<sup>2</sup> = H

**1c:** R<sup>1</sup> = CH<sub>2</sub>NHTs, R<sup>2</sup> = H

**1d:** R<sup>1</sup> = C<sub>6</sub>H<sub>4</sub>-4-C<sub>6</sub>H<sub>5</sub>, R<sup>2</sup> = H

**1e:** R<sup>1</sup> = C<sub>6</sub>H<sub>5</sub>, R<sup>2</sup> = C<sub>6</sub>H<sub>5</sub>

**1f:** R<sup>1</sup> = C<sub>6</sub>H<sub>5</sub>, R<sup>2</sup> = CH<sub>2</sub>NHTs

**1g:** R<sup>1</sup> = *n*-C<sub>5</sub>H<sub>11</sub>, R<sup>2</sup> = CH<sub>2</sub>NHTs

**1h:** R<sup>1</sup> = C<sub>6</sub>H<sub>5</sub>, R<sup>2</sup> = CH<sub>2</sub>OBn

**1i:** R<sup>1</sup> = 4-CH<sub>3</sub>COC<sub>6</sub>H<sub>4</sub>, R<sup>2</sup> = *n*-C<sub>4</sub>H<sub>9</sub>

**1j:** R<sup>1</sup> = *n*-C<sub>6</sub>H<sub>13</sub>, R<sup>2</sup> = CO<sub>2</sub>Me

**1k:** R<sup>1</sup> = C<sub>6</sub>H<sub>5</sub>, R<sup>2</sup> = CO<sub>2</sub>Et

**1l:** R<sup>1</sup> = CO<sub>2</sub>Me, R<sup>2</sup> = CO<sub>2</sub>Me

entry	1	method	T (°C)	time (h)	alkene 2	conversion (%)	yield (%) <sup>b</sup>	Z/E <sup>c</sup>
1	1a	A	35	3	2a	100	(96)	
2	1a	B	35	6	2a	100	(91) <sup>d</sup>	
3	1b	A	80	1	2b	<10	trace	
4	1b	B	80	8	2b	100	(98) <sup>e</sup>	
5	1c	A	55	8	2c	100	93	
6	1c	B	55	8	2c	100	91	
7	1d	A	55	8	2d	100	(67) <sup>f</sup>	
8	1d	B	55	8	2d	100	90	
9 <sup>g</sup>	1e	A	80	5	2e	100	(86)	100/0
10 <sup>h,i</sup>	1e	B	80	5	2e	100	85	100/0
11 <sup>g</sup>	1f	A	55	5	2f	100	96	100/0
12 <sup>g</sup>	1f	B	55	32	2f	92	(92)	100/0
13 <sup>g</sup>	1g	A	80	8	2g	100	81	100/0
14 <sup>h</sup>	1g	B	80	3	2g	40	(40)	100/0
15 <sup>g</sup>	1h	A	80	2.5	2h	78	(78)	100/0
16 <sup>h</sup>	1h	B	80	12	2h	60	(60)	100/0
17	1i	A	80	3	2i	100	(93)	100/0
18	1i	B	80	3	2i	100	98	100/0
19	1j	A	35	5	2j	100	95	100/0
20	1j	B	35	11	2j	100	(85)	100/0
21 <sup>h</sup>	1k	A	35	10	2k	100	90	>99/1
22 <sup>h</sup>	1k	B	35	15	2k	100	90	100/0
23 <sup>g</sup>	1l	B <sup>j</sup>	25	1.5	2l	100	(80)	100/0

<sup>a</sup>Conditions: AuNPore (2 mol %), alkyne (0.5 mmol), PhMe<sub>2</sub>SiH (0.75 mmol), H<sub>2</sub>O (1 mmol); method A, DMF (1 M); method B, pyridine (0.25 mmol), CH<sub>3</sub>CN (1 M). <sup>b</sup>Isolated yield. <sup>1</sup>H NMR yield determined using CH<sub>2</sub>Br<sub>2</sub> as an internal standard is shown in parentheses. <sup>c</sup>E/Z ratio was determined by H NMR spectroscopy. <sup>d</sup>Over-reduced product was obtained in 9% yield. <sup>e</sup>Pyridine (0.5 mmol) was used. <sup>f</sup>Over-reduced product was obtained in 33% yield. <sup>g</sup>PhMe<sub>2</sub>SiH (1.5 mmol) and H<sub>2</sub>O (1.75 mmol) were used. <sup>h</sup>PhMe<sub>2</sub>SiH (1.0 mmol) and H<sub>2</sub>O (1.25 mmol) were used. <sup>i</sup>Pyridine (0.35 mmol) was used. <sup>j</sup>The reaction was carried out in the absence of pyridine.

with a small amount of the recovered **1b** without formation of the over-reduced alkane (entry 5). Interestingly, we did not observe an obvious H<sub>2</sub> evolution in the presence of amines, but in the absence of amines, the reaction liberated a vigorous gas, giving **2b** in a very poor yield (entry 6), indicating that the use of amines effectively suppressed the formation of H<sub>2</sub> gas, resulting in a significantly increased reaction efficiency. To investigate the influence of the amount of pyridine on reaction efficiency, further optimization was performed by changing the equivalent of pyridine. Reducing the equivalents of pyridine from 0.5 to 0.2 resulted in a lower yield of **2b** from 84% to 78% (entries 5 and 7). Increasing the equivalent of pyridine to 1.0 afforded **2b** in 98% yield, while the use of 1.5 equiv of pyridine resulted in a decreased yield (entries 8 and 9). These results indicate that the use of proper amounts of pyridine efficiently suppresses the association of hydrogen atoms, which are able to reduce alkyne to alkene in high yield. The catalytic loading can be reduced to 0.2 mol % without any influence on chemical yield and chemoselectivity of **2a**, while the prolonged reaction time is needed (45 h, entry 10).

**Scope of Alkynes in AuNPore-Catalyzed Semihydrogenation.** The catalytic activity of AuNPore was further

examined with various terminal and internal alkynes under the aforementioned two methods: DMF as solvent (method A) and pyridine (0.5 equiv) in CH<sub>3</sub>CN (method B), except where noted (Table 4). The efficiency and chemoselectivity toward alkynes over alkenes of the present semihydrogenation are highly dependent on the used methods (A or B) and substituents at the alkynyl terminus. Relative to the high yield and no over-reduction for semihydrogenation of phenyl acetylene (**1a**) under method A, 9% of over-reduced alkane was obtained together with the desired styrene **2a** under method B (entries 1 and 2). In contrast, the aliphatic terminal alkyne, dodec-1-yne (**1b**), gave a poor conversion with evolution of H<sub>2</sub> gas under the method A, while an excellent yield and chemoselectivity of the desired alkene **2b** were observed under method B (80 °C) (entries 3 and 4). Among the other terminal alkynes tested, both methods A and B (55 °C) are suitable for chemoselective semihydrogenation of the *N*-tosyl-protected propargylamine **1c**, giving the corresponding alkene **2c** in high yields without formation of any over-reduced product (entries 5 and 6). Although the biphenyl-substituted acetylene **1d** reacted selectively under method B to give the desired alkene **2d** in 90% isolated yield,

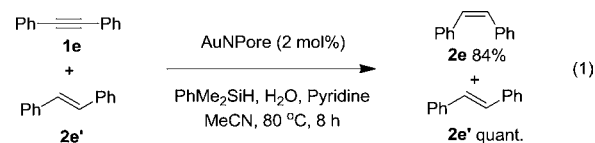


a high proportion of over-reduced alkane was observed with method A (entries 7 and 8).

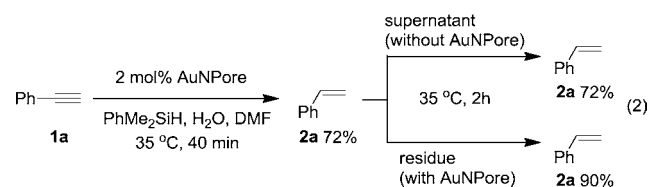
To further explore the stereoselectivity, we examined several simple and functionalized internal alkynes. 1,2-Diphenylethyne (**1e**) is a suitable substrate for the present hydrogenation, providing the exclusive (*Z*)-stilbene (**2e**) in 85% yield under the method A or B at 80 °C, which was difficult to obtain in high *Z*-selectivity in the case of Pd catalysts (entries 9 and 10).<sup>15</sup> Note that 1,2-dialkyl-substituted internal alkyne such as dodec-6-yne did not participate in the present reaction conditions. During further investigation of other hydrosilanes having a strong hydride source, we found that the use of (EtO)<sub>3</sub>SiH instead of PhMe<sub>2</sub>SiH under both methods A and B gave almost quantitative yield of (*Z*)-dodec-6-ene. However, there is a problem on reproducibility of the reaction, probably due to the formation of an unknown turbid emulsion mixture during the reaction; sometimes the yield of (*Z*)-dodec-6-ene decreased dramatically. Hydrogenations of the functionalized alkynes were also tested. The reactions of *N*-tosyl-protected propargylamines bearing phenyl (**1f**) or *n*-pentyl (**1g**) substituent at the alkynyl terminus afforded the corresponding *Z*-alkenes **2f** and **2g** as a sole product in good to high yield under method A, respectively (entries 11 and 13), while the relatively lower conversion yields were observed under method B, especially for the reaction of **1g** (entries 12 and 14). Benzyl ethers are known to undergo hydrogenolysis of benzyl group in the presence of H<sub>2</sub>/Pd-C.<sup>16</sup> Our methods A and B show a remarkable selectivity at the alkyne moiety for reducing the benzyl-protected propargyl alcohol **1h** without cleavage of benzyl group, giving the desired *Z*-alkene **2h** in 78% and 60% yields, respectively (entries 15 and 16). A remarkable chemoselectivity toward semihydrogenation of the alkyne group only has been observed with the alkyne **1i** bearing a ketone functional group on benzene ring, which produced the desired *Z*-alkene **2i** in excellent yield without reduction of carbonyl group (entries 17 and 18).<sup>13c</sup> It is known that the hydrogenation of  $\alpha,\beta$ -unsaturated alkynyl esters gave the high amounts of the thermodynamically more stable *E*-alkenes in the presence of Pd catalysts.<sup>17</sup> Our method exhibits excellent *Z*-selectivity with hydrogenation of  $\alpha,\beta$ -unsaturated alkynyl esters. The reaction of **1j** having *n*-hexyl group at the alkynyl terminus proceeded at 35 °C, giving the *Z*-alkene **2j** in high yield with 100% *Z*-selectivity under method A, while a lower conversion was observed under method B (entries 19 and 20). Methyl 3-phenylpropionate (**1k**) was also successfully hydrogenated to afford the desired *Z*-alkene **2k** in 90% isolated yield under methods A and B (entries 21 and 22). It is noteworthy that the electron-poor alkyne dimethyl butynedioate (**1l**) is highly reactive; the reaction proceeded in the absence of pyridine under method B to afford the desired dimethyl maleate (**2l**) as a sole product in 80% yield (entry 23), while **1l** was decomposed in the presence of pyridine in method B or under method A. For the examples with less than 90% yield in Table 4, <sup>1</sup>H NMR and GC-MS of the crude reaction mixture showed no byproduct formation unless otherwise noted.

**Control Experiments and Reaction Pathways.** Several control experiments were conducted to understand the catalytic activity and selectivity that may support our proposed mechanism. As shown in eq 1, the reaction of a 1:1 mixture of diphenylethyne (**1e**) and *E*-stilbene under method B gave the corresponding *Z*-stilbene **2e** in 84% yield along with the recovered *E*-stilbene in quantitative yield without any formation of over-reduced alkane. This result indicates that the AuNPore

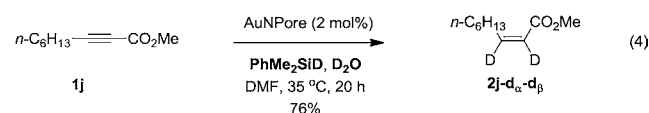
catalyst has a preferential chemoselectivity for alkynes over alkenes, which is consistent with the reported theoretical and experimental results that Au leads to the exothermic absorption for alkynes and endothermic absorption for alkenes.<sup>11a,18</sup>



To clarify whether the AuNPore catalyst leached into the reaction mixture or not, we carried out the following leaching experiments (eq 2). Phenyl acetylene **1a** was treated with PhMe<sub>2</sub>SiH and water in the presence of AuNPore catalyst (2 mol %) in DMF at 35 °C (method A). After 40 min, a part of the supernatant was transferred to the other reaction vessel, and **2a** was produced in 72% yield at this time. The supernatant was continuously heated at 35 °C in the absence of the catalyst for 2 h, affording **2a** in 72% yield. In contrast, the residual containing the AuNPore catalyst was completed in 2 h, giving **2a** in 90% yield. These results clearly indicated that the present hydrogenation was catalyzed by the solid state of AuNPore without any leaching of gold.



To gain further insight into reaction details, we carried out the deuterium labeling experiments. The reaction of alkyne **1i** with PhMe<sub>2</sub>SiH and D<sub>2</sub>O in the presence of AuNPore catalyst in DMF gave a 4:1 mixture of the corresponding  $\alpha$ -D- and  $\beta$ -D-incorporated *Z*-alkenes **2j-d<sub>α</sub>** and **2j-d<sub>β</sub>** in 80% yield (eq 3). The hydrogen derived from PhMe<sub>2</sub>SiH and deuterium derived from D<sub>2</sub>O are preferentially attached to the  $\beta$ - and  $\alpha$ -positions of  $\alpha,\beta$ -unsaturated alkenyl ester to give **2j-d<sub>α</sub>** as a major product and the hydrogen and deuterium exchanged alkene **2j-d<sub>β</sub>** as a minor product. When PhMe<sub>2</sub>SiD and D<sub>2</sub>O were used, the corresponding **2j-d<sub>α</sub>-d<sub>β</sub>** having two D atoms at both  $\alpha$ - and  $\beta$ -positions was obtained in 76% yield (eq 4). These results clearly indicate that the hydrogen atoms on *Z*-alkene moiety in product **2** were derived from PhMe<sub>2</sub>SiH and water, and the product proportion of **2j-d<sub>α</sub>** and **2j-d<sub>β</sub>** suggests the two reaction pathways: ionic and atomic hydrogenations (vide infra).<sup>19</sup>

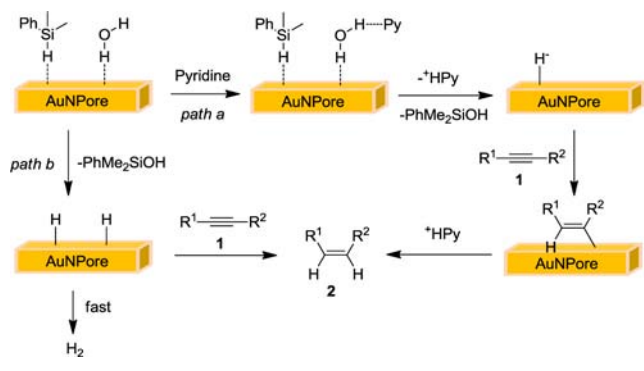


To investigate the interaction between pyridine and AuNPore, the pyridine-treated AuNPore was characterized using XPS analysis as shown in Figure 2b vs c. The XPS of Au 4f 7/2 is slightly shifted to the higher binding energy as compared to the fresh AuNPore. However, this difference is very small, indicating that the interaction between pyridine and

AuNPore surface is weak. Furthermore, we found that, when pyridine was treated with water in acetonitrile solution, a strong broad band appeared at  $3594\text{ cm}^{-1}$  in the FTIR spectrum, which is assigned as stretching vibration of  $\text{-OH}$  in the pyridine–water complex.<sup>20</sup> However, the water in acetonitrile and pyridine in acetonitrile did not show clear vibration in the same region (Figure S2). These results suggest the strong interaction between pyridine and water through hydrogen-bond formation.

On the basis of these experimental observations, two reaction pathways, ionic and atomic hydrogenations, are conceivable for the present catalytic semihydrogenation as shown in Scheme 2.

**Scheme 2. Reaction Pathways for the AuNPore-Catalyzed Semihydrogenation of Alkynes**



Initially,  $\text{PhMe}_2\text{SiH}$  and  $\text{H}_2\text{O}$  get absorbed onto the low-coordinated Au atoms on the stepped surface of AuNPore catalyst. In path a, the hydrogen bond forms between pyridine and water followed by the reaction of hydrosilane and water to give  $[\text{AuNPore-H}]^-$  and  $[\text{HPy}]^+$  species. Next, the adsorbed alkyne reacts subsequently with  $[\text{AuNPore-H}]^-$  and  $[\text{HPy}]^+$  to form the corresponding Z-alkene. In contrast, as shown in path b, the reaction of the adsorbed hydrosilane and  $\text{H}_2\text{O}$  forms hydrogen atom on AuNPore surface. In the absence of amines, the hydrogen atom may rapidly associated together to liberate  $\text{H}_2$  gas, which inhibits the hydrogenation of alkyne to afford low yield of the desired alkene. Note that in the case of method A, the formed hydrogen atoms may reduce DMF to produce some amounts of  $\text{Me}_2\text{NH}$  or/and  $\text{Me}_3\text{N}$ , which act as amine base. We conclude that the ionic hydrogenation (path a) is the predominant pathway in the present semihydrogenation, which suppresses  $\text{H}_2$  formation sufficiently in the presence of amines. In addition, the lower adsorption ability of the alkene on gold catalyst as compared to the alkyne inhibits its further hydrogenation to the alkane, leading to high chemoselectivity.

## CONCLUSION

In summary, we have shown for the first time that the unsupported AuNPore catalyst is an efficient heterogeneous catalyst for the selective semihydrogenation of alkynes, whereas the unsupported gold was known to be inactive for hydrogenation so far. The labeling experiments clearly indicated that organosilanes and water were the hydrogen source. The use of DMF as a solvent that generates amines in situ, or pyridine as an additive, is required to suppress the formation of  $\text{H}_2$ , leading to the efficient semihydrogenation. A wide range of terminal and internal alkynes can be reduced to the Z-alkenes in high yields with excellent chemo- and stereoselectivity. Moreover, the AuNPore catalyst is easily recoverable and can be reused several times without leaching and loss of activity. TEM characterization revealed that the AuNPore

catalyst has a bicontinuous 3D structure and atomic steps and kinks on ligament surfaces with a high concentration of low-coordinated Au atoms, which should be one of the important origins of catalytic activity. Further extension of this hydrogenation method to other unsaturated multiple bonds is in progress.

## EXPERIMENTAL SECTION

**General Information.** GC–MS analysis was performed on an Agilent 6890N GC interfaced to an Agilent 5973 mass-selective detector ( $30\text{ m} \times 0.25\text{ mm}$  capillary column, HP-5MS). Scanning electron microscope (SEM) observation was carried out using a JEOL JSM-6500F instrument operated at an accelerating voltage of 30 kV. TEM characterization was performed using a JEM-2100F TEM (JEOL, 200 kV) equipped with double spherical aberration (Cs) correctors for both the probe-forming and the image-forming lenses. The XPS measurements were carried out using a VG ESCALAB 250 spectrometer (Thermo Fisher Scientific K.K.) employing monochromatic Al K X-ray radiation. The base pressure of the analysis chamber was less than  $10^{-8}$  Pa.  $^1\text{H}$  NMR and  $^{13}\text{C}$  NMR spectra were recorded on JEOL JNM AL 400 (400 MHz) spectrometers.  $^1\text{H}$  NMR spectra are reported as follows: chemical shift in ppm ( $\delta$ ) relative to the chemical shift of  $\text{CDCl}_3$  at 7.26 ppm, integration, multiplicities ( $s$  = singlet,  $d$  = doublet,  $t$  = triplet,  $q$  = quartet,  $m$  = multiplet, and  $br$  = broadened), and coupling constants (Hz).  $^{13}\text{C}$  NMR spectra were recorded on JEOL JNM AL 400 (100.5 MHz) spectrometers with complete proton decoupling, and chemical shift was reported in ppm ( $\delta$ ) relative to the central line of triplet for  $\text{CDCl}_3$  at 77 ppm. IR spectra were recorded on a JASCO FT/IR-4100 spectrometer; absorptions are reported in  $\text{cm}^{-1}$ . High-resolution mass spectra were obtained on a BRUKER APEXIII spectrometer and JEOL JMS-700 MStation operator. Column chromatography was carried out employing silica gel 60 N (spherical, neutral, 40–100  $\mu\text{m}$ , KANTO Chemical Co.). Analytical thin-layer chromatography (TLC) was performed on 0.2 mm pre-coated plate Kieselgel 60 F254 (Merck).

**Materials.** The hydrosilanes and alkynes are commercially available, which are used as received. Au (99.99%) and Ag (99.99%) are purchased from Tanaka Kikinzoku Hanbai K.K. and Mitsuwa's Pure Chemicals, respectively. Structures of the known products were identified by  $^1\text{H}$ ,  $^{13}\text{C}$  NMR, and GC–MS as compared to the reported authentic compounds. The new products were confirmed by  $^1\text{H}$ ,  $^{13}\text{C}$  NMR, and HRMS (see the Supporting Information).

**Fabrication of AuNPore Catalyst.** Au (99.99%) and Ag (99.99%) were melted with electric arc-melting furnace under Ar atmosphere to form Au/Ag alloy (30:70, in at. %), which was rolled down to thickness of 0.04 mm. The resulting foil was annealed at 850  $^\circ\text{C}$  for 20 h. The foil was cut into small pieces ( $5 \times 2\text{ mm}$  square). Treatment of the resulting chips (67.1 mg) with 70 wt % nitric acid (3.77 mL) for 18 h at room temperature in a shaking apparatus resulted in the formation of the nanoporous structure by selective leaching of silver. The material was washed with a saturated aqueous solution of  $\text{NaHCO}_3$ , pure water, and acetone, successively. Drying of the material under reduced pressure gave the nanoporous gold (30.2 mg), and its composition was found to be  $\text{Au}_{98}\text{Ag}_2$  from EDX analysis.

**Representative Procedure for the AuNPore-Catalyzed Semihydrogenation of 1j (Table 4, Entry 19): Method A.** To a DMF solution (1 M, 0.5 mL) of AuNPore (2 mol %, 2.0 mg) were added 1j (84 mg, 0.5 mmol),  $\text{H}_2\text{O}$  (18  $\mu\text{L}$ , 1.0 mmol), and  $\text{PhMe}_2\text{SiH}$  (116  $\mu\text{L}$ , 0.75 mmol) subsequently at room temperature. The reaction mixture was stirred at 35  $^\circ\text{C}$  for 5 h and was monitored by GC–MS analysis. The AuNPore catalyst was recovered by filtration, and the solution was extracted with diethyl ether and washed with water. The recovered AuNPore catalyst was washed with acetone and dried under a vacuum. After concentration, the residue was purified with silica gel chromatography to afford 2j (81 mg, 95%) as a yellow solid.

**Representative Procedure for the AuNPore-Catalyzed Semihydrogenation of 1d (Table 4, Entry 8): Method B.** To a  $\text{CH}_3\text{CN}$  solution (1 M, 0.5 mL) of AuNPore (2 mol %, 2.0 mg) were added 1d (89 mg, 0.5 mmol),  $\text{H}_2\text{O}$  (18  $\mu\text{L}$ , 1.0 mmol), pyridine (20  $\mu\text{L}$ , 0.25 mmol), and  $\text{PhMe}_2\text{SiH}$  (116  $\mu\text{L}$ , 0.75 mmol). The reaction mixture

was stirred at 55 °C for 8 h. The reaction was monitored by GC–MS analysis. The mixture was filtered and washed with diethyl ether. The recovered AuNPore catalyst was washed with acetone and dried under a vacuum. After concentration of the filtrate, the residue was purified with a silica gel chromatography, to afford **2d** (81 mg, 90%) as a white solid.

## ■ ASSOCIATED CONTENT

### ■ Supporting Information

Experimental procedures and characterization data. This material is available free of charge via the Internet at <http://pubs.acs.org>.

## ■ AUTHOR INFORMATION

### Corresponding Author

tjin@m.tohoku.ac.jp

### Present Address

<sup>||</sup>Taketoshi Minato, Office of Society-Academia Collaboration for Innovation, Kyoto University Gokasho, Uji, Kyoto 611-0011, Japan.

### Notes

The authors declare no competing financial interest.

## ■ ACKNOWLEDGMENTS

This work was supported by Scientific Research (A) from Japan Society for Promotion of Science (JSPS) (No. 23245020), and World Premier International Research Center Initiative (WPI), MEXT, Japan. M.Y. acknowledges the support of the China Scholarship Council (CSC). We thank Dr. Aiko Nakao (Cooperative Support Team, RIKEN Advanced Science Institute) for assistance with the XPS experiments.

## ■ REFERENCES

- (1) For CO oxidation, see: (a) Zielasek, V.; Jürgens, B.; Schulz, C.; Biener, J.; Biener, M. M.; Hamza, A. V.; Bäumer, M. *Angew. Chem., Int. Ed.* **2006**, *45*, 8241. (b) Xu, C.; Su, J.; Xu, X.; Liu, P.; Zhao, H.; Tian, F.; Ding, Y. *J. Am. Chem. Soc.* **2007**, *129*, 42. (c) Xu, C.; Xu, X.; Su, J.; Ding, Y. *J. Catal.* **2007**, *252*, 243. (d) Wittstock, A.; Neumann, B.; Schaefer, A.; Dumbuya, K.; Kübel, C.; Biener, M. M.; Zielasek, V.; Steinrück, H. P.; Gottfried, J. M.; Biener, J.; Hamza, A.; Bäumer, M. *J. Phys. Chem. C* **2009**, *113*, 5593. (e) Wang, L. C.; Jin, H. J.; Widmann, D.; Weissmuller, J.; Behm, R. J. *J. Catal.* **2011**, *278*, 219.
- (2) (a) Wittstock, A.; Zielasek, V.; Biener, J.; Friend, C. M.; Bäumer, M. *Science* **2010**, *327*, 319. (b) Asao, N.; Hatakeyama, N.; Menggenbater; Minato, T.; Ito, E.; Hara, M.; Kim, Y.; Yamamoto, Y.; Chen, M.; Zhang, W.; Inoue, A. *Chem. Commun.* **2012**, *48*, 4540. (c) Yin, H.; Zhou, C.; Xu, C.; Liu, P.; Xu, X.; Ding, Y. *J. Phys. Chem. C* **2008**, *112*, 9673. (d) Kosuda, K. M.; Wittstock, A.; Friend, C. M.; Bäumer, M. *Angew. Chem., Int. Ed.* **2012**, *51*, 1698.
- (3) For electrochemical oxidation, see: (a) Zhang, J.; Liu, P.; Ma, H.; Ding, Y. *J. Phys. Chem. C* **2007**, *111*, 10382. (b) Yu, C.; Jia, F.; Ai, Z.; Zhang, L. *Chem. Mater.* **2007**, *19*, 6065. (c) Zeis, R.; Lei, T.; Sieradzki, K.; Snyder, J.; Erlebacher, J. *J. Catal.* **2008**, *253*, 132.
- (4) (a) Forty, A. *J. Nature* **1979**, *282*, 597. (b) Erlebacher, J.; Aziz, M. J.; Karma, A.; Dimitrov, N.; Sieradzki, K. *Nature* **2001**, *410*, 450.
- (5) (a) Hashmi, A. S. K.; Hutchings. *Angew. Chem., Int. Ed.* **2006**, *45*, 7896. (b) Pina, C. D.; Falletta, E.; Prati, L.; Rossi, M. *Chem. Soc. Rev.* **2008**, *37*, 2077. (c) Corma, A.; Garcia, H. *Chem. Soc. Rev.* **2008**, *37*, 2096. (d) Matsumoto, T.; Ueno, M.; Wang, N.; Kobayashi, S. *Chem.-Asian J.* **2008**, *3*, 196. (e) Corma, A.; Leyva-Pérez, A.; Sabater, M. *J. Chem. Rev.* **2011**, *111*, 1657.
- (6) Fujita, T.; Guan, P.; McKenna, K.; Lang, X.; Hirata, A.; Zhang, L.; Tokunaga, T.; Arai, S.; Yamamoto, Y.; Tanaka, N.; Ishikawa, Y.; Asao, N.; Yamamoto, Y.; Erlebacher, J.; Chen, M. *Nat. Mater.* **2012**, *11*, 775–780.

(7) (a) Bond, G. C.; Louis, C.; Thompson, D. T. *Catalysis by Gold*; Imperial College Press: London, 2006, Chapter 9, p 244. (b) McEwan, L.; Julius, M.; Roberts, S.; Fletcher, J. C. Q. *Gold Bull.* **2010**, *43*, 298.

(8) Fujitani, T.; Nakamura, I.; Akita, T.; Okumura, M.; Haruta, M. *Angew. Chem., Int. Ed.* **2009**, *48*, 9515.

(9) For recent selected homogeneous semihydrogenation of alkynes, see: (a) Hauwert, P.; Maestri, G.; Sprengers, J. W.; Catellani, M.; Elsevier, C. *J. Angew. Chem., Int. Ed.* **2008**, *47*, 3223. (b) La Pierre, H. S.; Arnold, J.; Toste, F. D. *Angew. Chem., Int. Ed.* **2011**, *50*, 3900. (c) Gianetti, T. L.; Tomson, N. C.; Arnold, J.; Bergman, R. G. *J. Am. Chem. Soc.* **2011**, *133*, 14904. (d) Shen, R.; Chen, T.; Zhao, Y.; Qiu, Y.; Zhou, Y.; Yin, S.; Wang, X.; Goto, M.; Han, L.-B. *J. Am. Chem. Soc.* **2011**, *133*, 17037.

(10) For selected heterogeneous semihydrogenation of alkynes, see: (a) Lindlar, H. *Helv. Chim. Acta* **1952**, *35*, 446. (b) Savoia, D.; Tagliavini, E.; Trombini, C.; Umani-Ronchi, A. *J. Org. Chem.* **1981**, *46*, 5340. (c) Brunet, J. J.; Caubere, P. *J. Org. Chem.* **1984**, *49*, 4058. (d) Gruttadauria, M.; Noto, R.; Deganello, G.; Liotta, L. F. *Tetrahedron Lett.* **1999**, *40*, 2857. (e) Gruttadauria, M.; Liotta, L. F.; Noto, R.; Deganello, G. *Tetrahedron Lett.* **2001**, *42*, 2015. (f) Alonso, F.; Osante, I.; Yus, M. *Adv. Synth. Catal.* **2006**, *348*, 305. (g) Hori, J.; Murata, K.; Sugai, T.; Shinohara, H.; Noyori, R.; Arai, N.; Kurono, N.; Ohkuma, T. *Adv. Synth. Catal.* **2009**, *351*, 3143. (h) Venkatesan, R.; Precht, M. H. G.; Scholten, J. D.; Pezzi, R. P.; Machado, G.; Dupont, J. *J. Mater. Chem.* **2011**, *21*, 3030. (i) Wu, J.; Wang, K.; Li, Y.; Yu, P. *Adv. Mater. Res.* **2011**, *233–235*, 2109. (j) Takahashi, Y.; Hashimoto, N.; Hara, T.; Shimazu, S.; Mitsudome, T.; Mizugaki, T.; Jitsukawa, K.; Kaneda, K. *Chem. Lett.* **2011**, *40*, 405.

(11) For the supported AuNPs-catalyzed semihydrogenation of alkynes, see: (a) Segura, Y.; López, N.; Pérez-Ramírez, J. *J. Catal.* **2007**, *247*, 383. (b) Jia, J.; Haraki, K.; Kondo, J. N.; Domen, K.; Tamaru, K. *J. Phys. Chem. B* **2000**, *104*, 11153. (c) Choudhary, T. V.; Sivadinarayana, C.; Datye, A. K.; Kumar, D.; Goodman, D. W. *Catal. Lett.* **2003**, *86*, 1. (d) Azizi, Y.; Petit, C.; Pitchon, V. *J. Catal.* **2008**, *256*, 338–344. (e) Nikolae, S. A.; Smirnov, V. V. *Catal. Today* **2009**, *147S*, S336.

(12) (a) Asao, N.; Ishikawa, Y.; Hatakeyama, N.; Menggenbater; Yamamoto, Y.; Chen, M.; Zhang, W.; Inoue, A. *Angew. Chem., Int. Ed.* **2010**, *49*, 10093. (b) Tanaka, S.; Kaneko, T.; Asao, N.; Yamamoto, Y.; Chen, M.; Zhang, W.; Inoue, A. *Chem. Commun.* **2011**, *47*, 5985. (c) Kaneko, T.; Tanaka, S.; Asao, N.; Yamamoto, Y.; Chen, M.; Zhang, W.; Inoue, A. *Adv. Synth. Catal.* **2011**, *353*, 2927. (d) Jin, T.; Yan, M.; Menggenbater; Minato, T.; Bao, M.; Yamamoto, Y. *Adv. Synth. Catal.* **2011**, *353*, 3095. (e) Asao, N.; Menggenbater; Seya, Y.; Yamamoto, Y.; Chen, M.; Zhang, W.; Inoue, A. *Synlett* **2012**, *23*, 66. (f) Asao, N.; Jin, T.; Tanaka, S.; Yamamoto, Y. *Pure Appl. Chem.* **2012**, *84*, 1771. (g) Jin, T.; Yan, M.; Yamamoto, Y. *ChemCatChem* **2012**, *4*, 1217.

(13) (a) Mohr, C.; Hofmeister, H.; Radnik, J.; Claus, P. *J. Am. Chem. Soc.* **2003**, *125*, 1905. (b) Corma, A.; Boronat, M.; Gonzalez, S.; Illas, F. *Chem. Commun.* **2007**, 3371. (c) Zhu, Y.; Qian, H.; Drake, B. A.; Jin, R. *Angew. Chem., Int. Ed.* **2010**, *49*, 1295.

(14) (a) Schreiner, S.; Yu, J. Y.; Vaska, L. *Inorg. Chim. Acta* **1988**, *147*, 139. (b) Sharma, H. K.; Panel, K. H. *Angew. Chem., Int. Ed.* **2009**, *48*, 7052. (c) Itazaki, M.; Ueda, K.; Nakazawa, H. *Angew. Chem., Int. Ed.* **2009**, *48*, 3313.

(15) Brunet, J. J.; Caubere, P. *J. Org. Chem.* **1984**, *49*, 4058.

(16) Heathcock, C. H.; Ratcliffe, R. *J. Am. Chem. Soc.* **1971**, *93*, 1746.

(17) Hönig, H.; Seuffer-Wasserthal, P.; Weber, H. *Tetrahedron* **1990**, *46*, 3841.

(18) Bridier, B.; López, N.; Pérez-Ramírez, J. *Dalton Trans.* **2010**, *39*, 8412.

(19) (a) Noujima, A.; Mitsudome, T.; Mizugaki, T.; Jitsukawa, K.; Kaneda, K. *Angew. Chem., Int. Ed.* **2011**, *50*, 2986. (b) Fang, M.; Machalaba, N.; Sánchez-Delgado, R. A. *Dalton Trans.* **2011**, *40*, 10621.

(20) Goethals, M.; Zeegers-Huyskens, T. *Spectrosc. Lett.* **1995**, *28*, 1125.